NUMERICAL INVESTIGATION OF EXTRUSION-BASED ADDITIVE MANUFACTURING FOR PROCESS PARAMETER PLANNING IN A POLYMER DISPENSING SYSTEM

Haiyang He[1,2], Bo Cheng[2,*], Kaja Schmidt[3,4], Claudia Kruse[3], Charles Tuffile[2]

[1]Department of Mechanical and Industrial Engineering
University of Illinois at Chicago
Chicago, Illinois 60607, USA
[2]Robert Bosch LLC, Cambridge, MA, 02139, USA
[3]Robert Bosch GmbH, Renningen, Stuttgart, 70465, GERMANY
[4]Institute of Micro Integration, University of Stuttgart, Stuttgart, 70569, GERMANY
*Corresponding author: Bo.Cheng@us.bosch.com

Abstract

This paper establishes a computational fluid dynamics (CFD) model using ANSYS Fluent for the time-pressure polymer dispensing process. The developed model simulates the process of liquid being applied on a substrate and predicts critical performance indexes, such as strand width and height, of the dispensing system. A mesh sensitivity analysis has been performed to identify the element size for achieving satisfactory accuracy and efficient computation time. The influences of material properties, such as surface tension and viscosity, on the simulation results were investigated. In addition, the effect of flow rate and nozzle translational speed on strand width were studied. The simulation results were validated against experimental measurements, and the model was demonstrated to be effective in predicting the strand width. Based on the simulations, a process map was constructed for process parameter planning and optimization.

Keywords: Polymer dispensing; Computational fluid dynamics (CFD); Strand; Process-quality map;

1. Introduction

Additive manufacturing (AM) processes, also known as 3D printing, are becoming more and more prevalent in practical applications. Polymers and metals are the most common types of AM materials, while polymers are amongst the least expensive and most widely used materials in commercial 3D printers [1]. The main polymer AM processes include vat photopolymerization [2, 3], material extrusion (fused deposition modeling (FDM), or fused filament fabrication (FFF)) [4], material jetting [5, 6] and fluid dispensing [7]. Among these techniques, fluid dispensing is one of the most important processes in electronics packaging and circuit assembly. In such a process, liquid polymer is dispensed by a nozzle/needle on the substrate according to pre-defined path and cured by UV light to form desired shape with homogenously filled layers, as depicted in Figure 1. There are three major types of fluid dispensing approaches: time-pressure, rotary screw and positive displacement. The advantages and limits of various fluid dispensing technologies are discussed in literature [8, 9]. Due to its flexibility for various applications and easy operation and

maintenance, the time-pressure fluid dispensing approach is the most widely used dispensing technology [10].
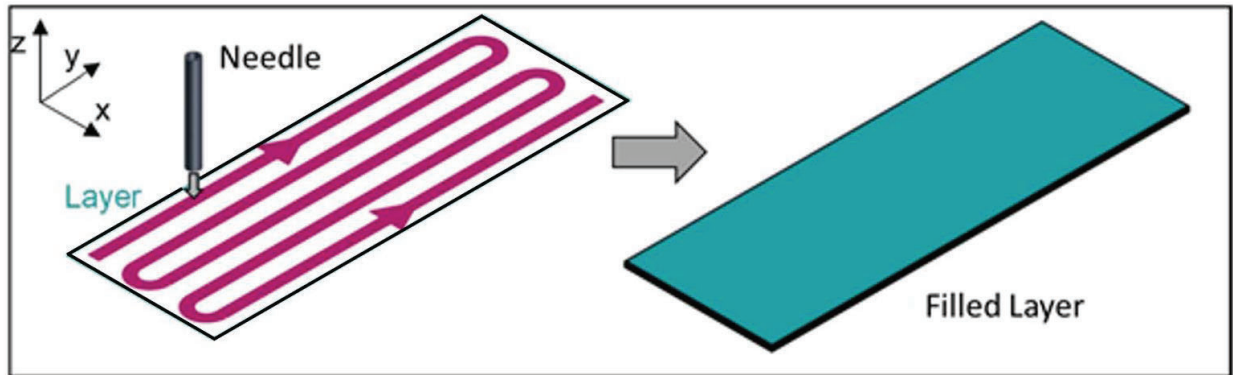

Fig. 1 Schematic of material dispensing in AM

Despite its wide application and success in electronics packaging, there are still many challenges to be addressed for time-pressure fluid dispensing. For instance, the flow rate of fluid dispensed and the shape of fluid beads formed on the substrate are difficult to represent [10], which makes control of this process a challenging task. The homogeneity of the filled layer is significantly affected by the process parameters in the fluid dispensing process. The primary process parameters include the material flow rate, nozzle translational speed, diameter of the nozzle, hatch spacing, standoff distance and material properties. Given multiple levels for each of above-mentioned parameters, the design space will grow exponentially. Thus, identifying the optimum parameter settings solely by an experimental approach will be challenging in terms of time, labor and cost. To increase the efficiency of identifying the optimum parameter settings for achieving the desired layer homogeneity, a numerical approach has been utilized for process simulation [11-15]. An analytical model for the time-pressure fluid dispensing process was established by Chen [10]. The flow rate, dispensed height and width can be predicted with this model. A stochastic framework for predicting the line width of the features deposited on the substrate, using a Monte Carlo probabilistic simulation, has been established by Vlasea [16]. A flash photography method for the measurements of the fluid flow dynamics in a fluid dispensing system was presented by Boonsang [17]. In a Fused Filament Fabrication (FFF) process, Heller et al [18] presented a computational model to simulate the extrusion shape of a polymer deposition planar flow field. The fiber orientation throughout the extruded nozzle and bead has been studied as well.

A commercial CFD package, ANSYS Fluent, is utilized in this paper to develop a numerical (CFD) model for the time-pressure polymer dispensing system. Sensitivity analysis has been performed for material properties, such as contact angle, surface tension and viscosity. Investigations have also been completed for flow rate and nozzle translational speed. Experimental validation has been carried out to demonstrate the effectiveness of the simulation model. Finally, the validated model is used for process parameter planning and optimization.

2. Experimental setup

Single track deposition experiment has been conducted to investigate process parameters effect in this study. A UV-heat curing adhesive (epoxy resin) was used as the deposition material. The dispensed material is then cured by UV light with a wavelength of 365 nm. An image of the dispenser is given in Fig. 2 (a). A built-in camera in the dispensing system, mounted on z-axis and perpendicular to build plate, is used to capture the images of the dispensed track. An example of the camera captured image is illustrated in Fig. 2 (b). The exemplary tracks clearly show variation in strand width during individual deposition, which is caused by non-ideal process parameters. For statistical analysis, five experimental replications were carried out for each set of experimental process parameters and the average strand width was used for experimental data analysis.

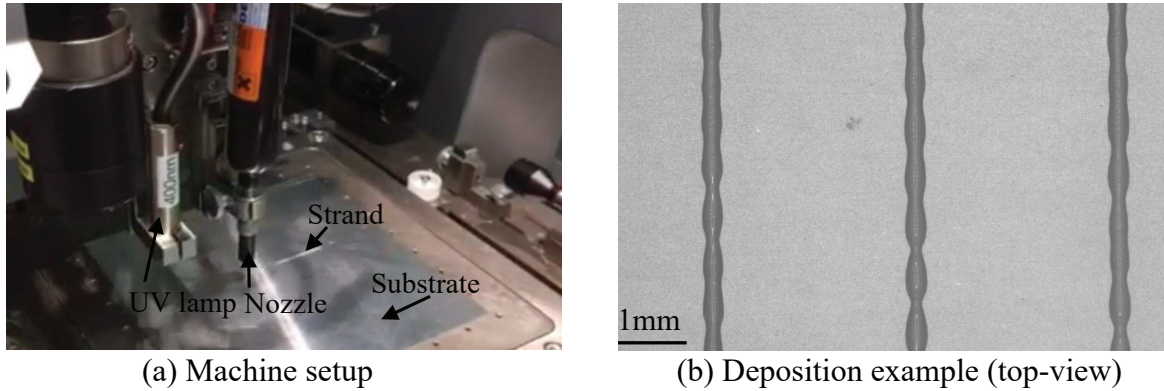| (a) Machine setup | (b) Deposition example (top-view) |

Fig. 2 Experimental setup

The primary parameters determining the geometry of the deposited strands include: material properties, nozzle diameter, standoff distance, flow rate and translational speed. In the experiment, a pressure-based system is used to "extrude" the material out of the nozzle, therefore, the actual flow rate is measured and calculated based on applied pressure. The values of the parameters for this study are shown in Table 1. They are some consistency issues observed for the flow rate in the parameter space, e.g., not exactly evenly distributed, especially between the one as small as 1.02 mm^3/s and other flow rates. During experiment, an even smaller flow rate may potentially lead to serious defect such as separate droplets, thus they are not included in this study.

Table 1 Parameters for the dispenser

Parameters	Value
Nozzle diameter (mm)	0.61
Surface tension (mN/m)	48.5
Viscosity (kg/m/s)	32
Standoff distance (mm)	0.2
Flow rate (mm^3/s)	1.02, 2.72, 5.07, 7.40, 9.97
Translational speed (mm/s)	24, 28, 32, 36, 40
Contact angle (°)	34

3. Modeling technique

A finite volume method (FVM) based CFD model has been established for the dispensing system using ANSYS Fluent. The deposition of the dispensed material is simulated as a Newtonian, incompressible and laminar fluid flow. The dynamics of the fluid material are calculated by the conservation of mass and momentum. The following assumptions have been made:

(1) A two phases (air and epoxy resin) CFD model was created. The simulation domain is initially filled with air, then the fluid entered the domain from the inlet nozzle with a given flow rate.
(2) A no slip condition exists for all surfaces, e.g., nozzle and substrate, to ensure that the liquid adheres to the surfaces.
(3) There is no temperature change in the experimental dispensing process, thus the whole simulation is considered isothermal.
(4) There is a UV-light curing process after the liquid dispensing process to ensure the solidification of dispensed material. The volume change during this process is very small, thus the effect of UV-light curing process on the volume is ignored. Only the fluid deposition process was modeled in this study.
(5) Instead of moving the nozzle, a translational speed is given to the substrate to simulate the process of material deposition.

ANSYS Fluent numerically solves the conservation equations for mass and momentum [19]. The equation for conservation of mass is:

$$\frac{\partial \rho}{\partial t} + \nabla \cdot (\rho \vec{v}) = S_m \tag{1}$$

Where ρ is the amount of the fluid per unit volume, t is time, ∇ is divergence, $\vec{v}$ is the flux of the fluid and S_m is the generation of the fluid per unit volume per unit time. Conservation of momentum is described by:

$$\frac{\partial (\rho \vec{v})}{\partial t} + \nabla \cdot (\rho \vec{v} \vec{v}) = -\nabla p + \nabla \cdot (\bar{\bar{\tau}}) + \rho \vec{g} + \vec{F} \tag{2}$$

Where p is the static pressure, $\bar{\bar{\tau}}$ is the stress tensor, $\rho \vec{g}$ and $\vec{F}$ are the gravitational body force and external body forces, respectively.

The free surface evolution of the deposition process is capture by volume of fluid (VOF) method. A cell without fluid is represented as F=0 while a cell fully filled with fluid is represented as F=1. Thus, a cell that is partially fluid is defined as 0 < F < 1. The VOF equation is:

$$\frac{\partial F}{\partial t} + \nabla \cdot (\vec{v} F) = 0 \tag{3}$$

An exemplary plot of the numerical model is represented in Fig. 3(a). The printing nozzle is modeled as a cylindrical tube with a fixed diameter. The moving substrate, with changeable translational speed, has a certain standoff distance from the printing nozzle. Fig. 3(b) shows the

geometrical and meshing information of the model. The mesh was refined in the nozzle region, e.g., 25% of the size of the elements in other regions. The single track deposition of dispensed material was simulated for different printing conditions, as shown in Table 1.
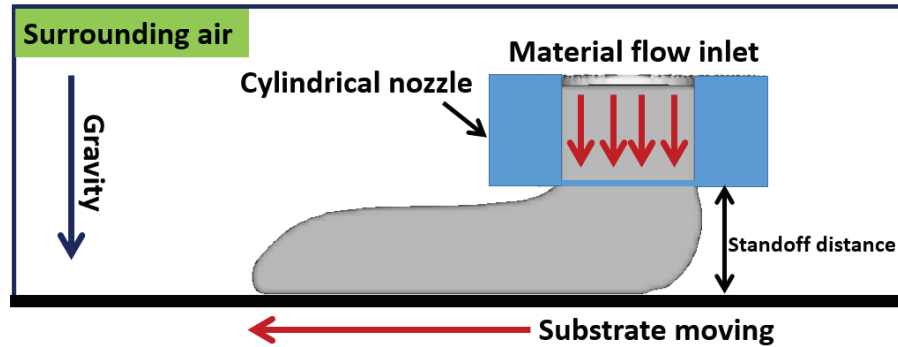
(a) Exemplary plot of the simulation model
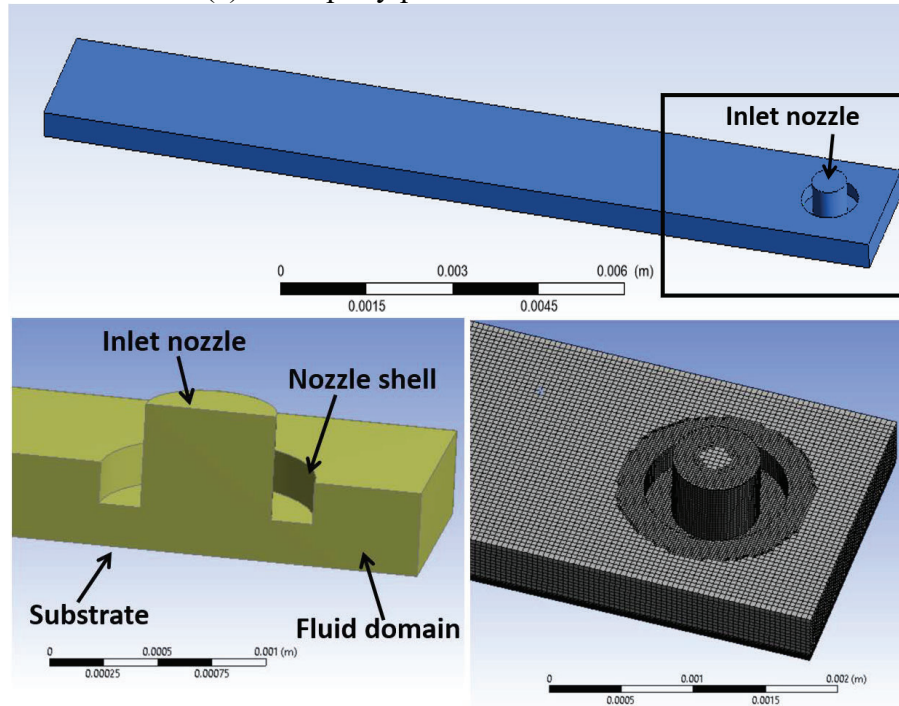
(b) Model geometrical and meshing information
Fig. 3 Construction of the simulation model

A mesh sensitivity study was performed to identify an appropriate mesh size which can strike a balance between computation time and accuracy. A line of material was deposited, and its width was extracted from the simulation results. Mesh sizes of 0.0031 cm, 0.0040 cm, 0.0050 cm, 0.0060 cm were tested. A translational speed of 24 mm/s and a flow rate of 2.72 mm^3/s were used in the model. The simulated results for each of the mesh sizes are shown in Fig. 4. It turns out that the simulation calculations converge well for mesh sizes of 31 µm, 40 µm and 50 µm. In addition, the simulation time will be drastically decreased (>50%) when changing the mesh size from 31 µm to 40 µm. Therefore, a mesh size of 40 µm was used for the subsequent simulations.
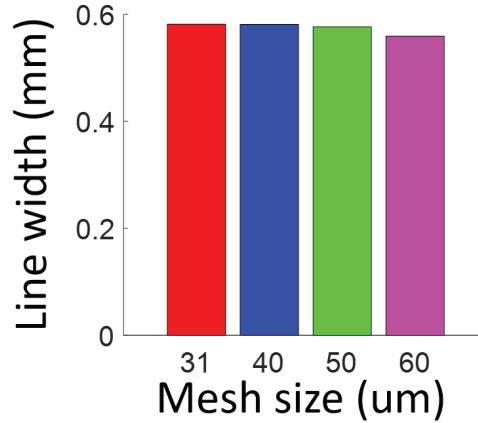
Fig. 4 Mesh sensitivity analysis

4. Results and discussion

4.1 Process parameters effect
4.1.1 Influence of translational speed

The shape of the deposited track was simulated by the VOF method. Fig. 5 shows examples of isotropic, top and side views of the deposited tracks for two printing process parameters: (a) 24 mm/s and 5.07 mm^3/s, (b) 40 mm/s and 5.07 mm^3/s. The red color region represents the inlet material flow while the green color region represents the deposited materials. Due to the no slip boundary condition, the material will adhere to the substrate once it touches the boundary surface. It can be observed that there is more fluid spread around the nozzle head for case (a), e.g., front and side area. Therefore, more deposited fluid material is pushed to the nozzle periphery under a slower translational moving speed, and a larger strand width is formed. A series of translational speeds have been simulated and the strand widths are concluded in Fig. 6. A linear relationship can be identified between the strand width and translational speed.
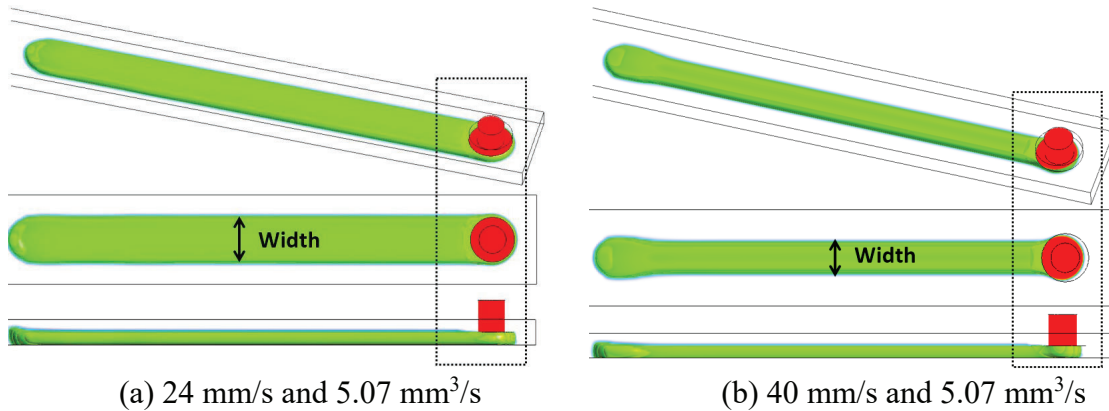

(a) 24 mm/s and 5.07 mm^3/s   (b) 40 mm/s and 5.07 mm^3/s
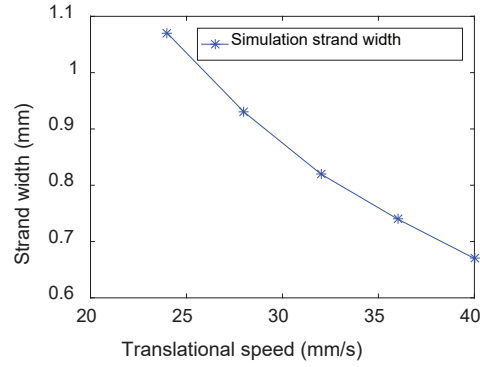Fig. 5 Simulation results for different translation speeds

Fig. 6 Strand width comparison for different translational speeds

4.1.2 Influence of flow rate

The effect of material flow rate was investigated by fixing the translational speed at 32 mm/s and varying the flow rate from 1.02 mm^3/s to 9.97 mm^3/s. The simulation results are depicted in Fig. 7, where it is apparent that a more homogeneous strand is achieved with the increase of flow rate conditions. There are clearly strand width variations along the deposition track for the 1.02 mm^3/s flow rate condition, as shown in Fig. 7 (a). The iterative large-small-large shaped strand width leads to an inhomogeneous (porous) filled layer, and potentially poor final part quality. On the other hand, a uniform strand width is formed if the flow rate is high enough, e.g., Fig. 7 (b). Fig. 8 shows that the strand width will increase linearly as the flow rate increases.
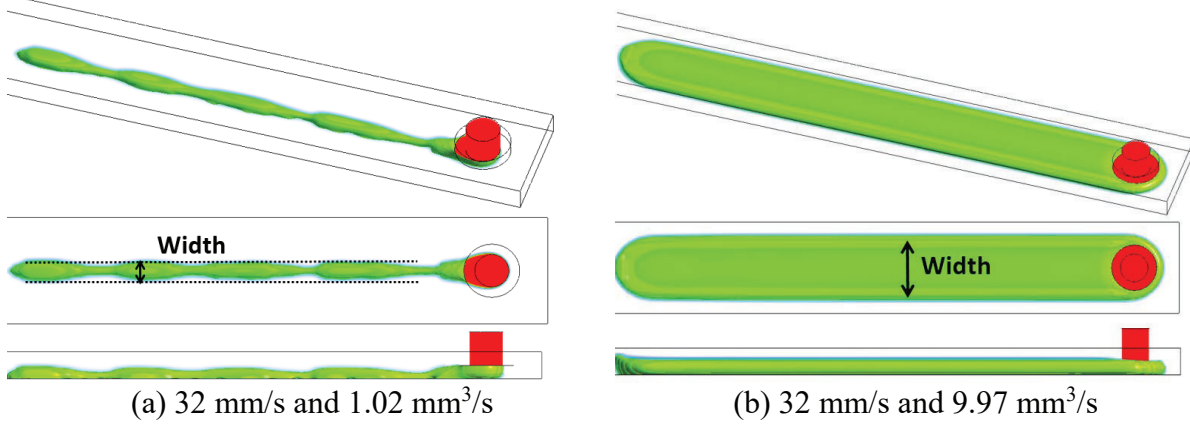

(a) 32 mm/s and 1.02 mm^3/s (b) 32 mm/s and 9.97 mm^3/s

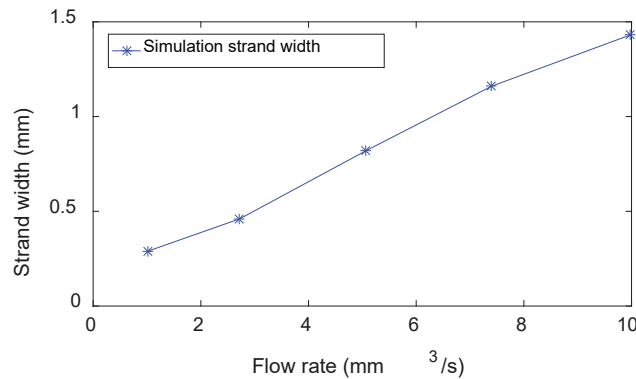Fig. 7 Simulation results for different flow rate

Fig. 8 Strand width comparison for different flow rate

4.2. Material property effect

To study the sensitivity of different material properties, a one-factor-at-a-time method has been used. Specifically, all of the parameters are set to the fixed values in Table 1 except the testing parameter. Therefore, the influence of three major material properties, namely contact angle, surface tension and viscosity, can be varied and tested individually. The translational speed and flow rate are set to be 24 mm/s and 2.72 mm^3/s.

Five different contact angle values were tested: 30º, 60 º, 90 º, 120 º, 150 º. A single line of material was deposited and the simulation results are plotted in Fig. 9 (a). There is a linear relationship between the simulated width and the contact angle. The slope of the fitting curve reveals the sensitivity of the simulated width to the variation of the contact angle.

Similar to the study for the influence of contact angle, four surface tension values, e.g., 30 mN/m, 60 mN/m, 90 mN/m and 120 mN/m, were studied. In addition, the surface tension module was turned off in one test case to show its effect. The simulation results are summarized in Fig. 9 (b). The red star marker represents the result of the case when the surface tension model is turned off. The application of the surface tension model produces a narrower strand, e.g., a clear trend is shown that the increase of the surface tension value decreases the strand width.
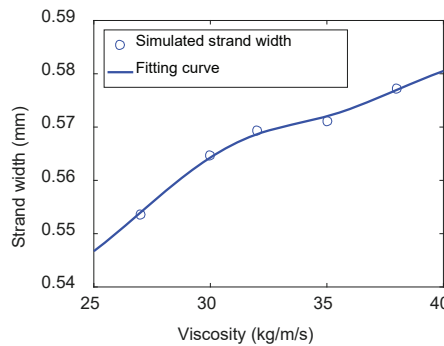
Finally, the following viscosity values were evaluated: 27 kg/m/s, 30 kg/m/s, 32 kg/m/s, 35 kg/m/s and 38 kg/m/s. Fig. 9 (c) presents the simulation results. It turns out that the viscosity values have a positive impact on the strand width, e.g., increase of viscosity value leads to an increase of the strand width.
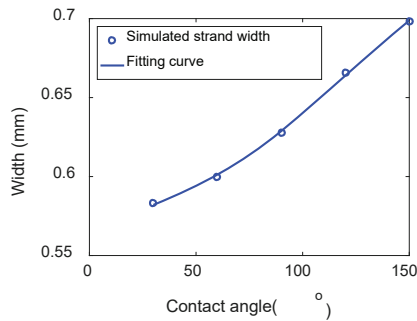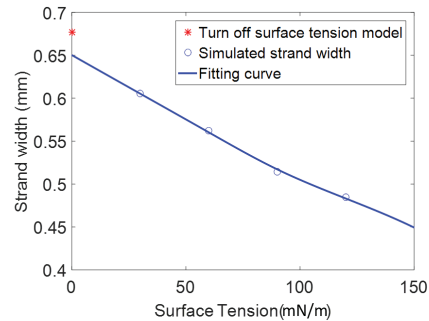
(a) Influence of contact angle   (b) Influence of surface tension

(c) Influence of viscosity

Fig. 9 Summary of material properties effect

4.3. Construction of process-quality map

Two process parameters, nozzle translational speed and flow rate, are utilized as inputs to create a process-quality map in this study. The translational speeds are 24 mm/s, 28 mm/s, 32 mm/s, 36 mm/s and 40 mm/s. The flow rates are 1.02 mm³/s, 2.72 mm³/s, 5.07 mm³/s, 7.40 mm³/s, 9.97 mm³/s. Thus, a total of 25 simulations have been performed for a full factorial design with 2 factors and 5 levels. The strand width condition is used as targeted output. Fig. 10 summarizes all of the simulated tracks. In the given process space, it was observed that the inhomogeneous deposited tracks were formed for a flow rate of 1.02 mm³/s, while a curved strand top surface can be formed for a combination of low speed and high flow rate. Only the process parameters that can generate homogeneous strands without a curved top surface are considered as suitable sets. The parameter sets inside the red line region (comfort zone) are recognized as reasonable parameter sets.
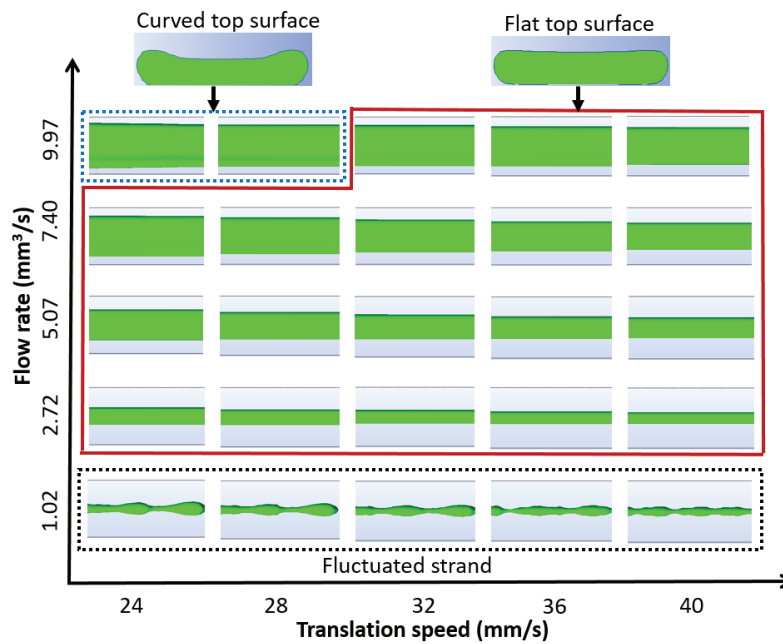

Fig. 10 Summary of all simulated tracks

Based on the simulation results, a 3D surface plot can be produced, e.g., strand width against flow rate and translational speed. In addition, a horizontal plane, which represents a desired width of the strand, can be used to intersect the 3D surface plot and generate an intersection contour. A projection of this curve can be projected to the 2D flow rate - translational speed plane. In this example, a horizontal plane with z level (strand width) of 0.8 mm is generated and intersects with the 3D surface plot. The exemplary intersection points and curve, colored in red, are obtained, as shown in Fig. 11. Therefore, for this certain model, given a desired strand width, the relationship between the nozzle flow rate and the nozzle translational speed should follow the intersection contour. Similar process maps involving various other process parameters can be constructed using this approach as well, which will increase the efficiency of experimental design.
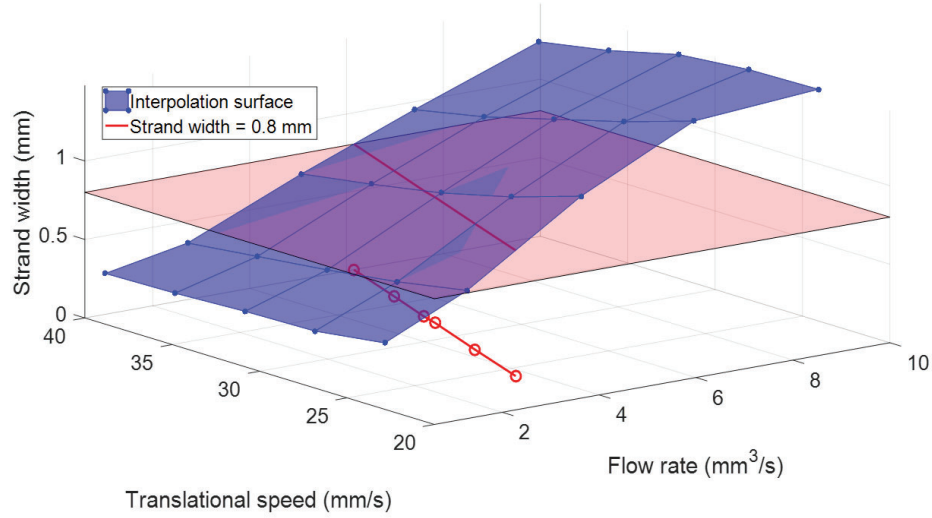
Fig. 11 Exemplary plot of process map generation

With the consideration of strand quality, a process-quality map can be generated by combining the strand quality space (Fig. 10) and the process map (Fig. 11). Fig. 12 presents an example of the generated process-quality map. The blue line is the strand width = 0.8 mm process curve, it falls in the comfort zone, which means that strands generated by different process parameter sets will not have defects such as inhomogeneous width or a curved strand top surface. On the other hand, the grey line with a strand width = 0.4 mm, which is across the defect zone and comfort zone, will have potential strand width fluctuation defect when lower translational speed and flow rate are used.
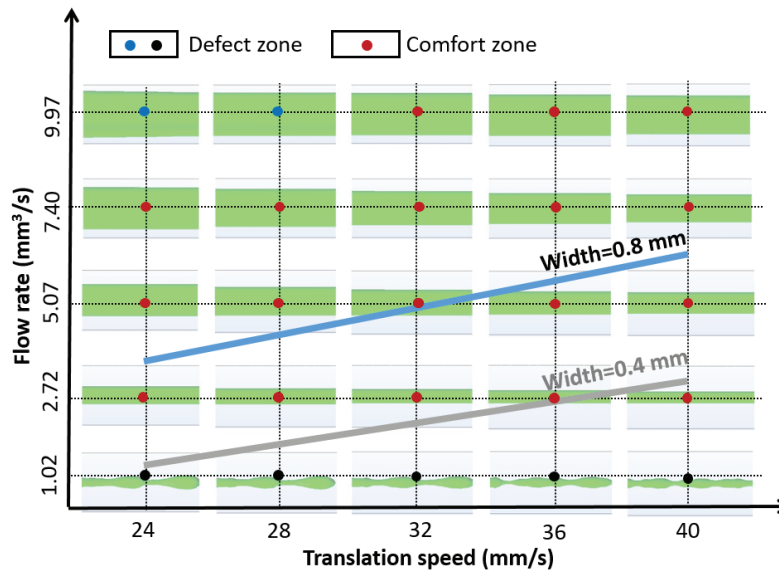

Fig. 12 Process-quality map

5. Experimental validation

The simulation results from the developed CFD model were validated against experimental results. Two process parameters, nozzle translational speed and flow rate, were investigated in this

study with the values specified in Table 1. A full factorial design with 2 factors and 5 levels was created and each design was replicated 5 times. In each experiment, a line of material was deposited, and the built-in camera of the dispenser machine measured the width of the strand. The average value was taken for each set of 5 replications so there are 25 widths in total for analysis. The comparison between the simulated and experimental results are presented in Fig. 13. For all of the simulated strand width, the maximum error is ~37% and the minimum error is ~2.4%. Overall, the established CFD model gives a reasonable prediction of the experiments. The error may be introduced by the material properties, e.g., surface tension, viscosity and contact angle. More material property measurements will be needed in future studies to improve simulation accuracy.
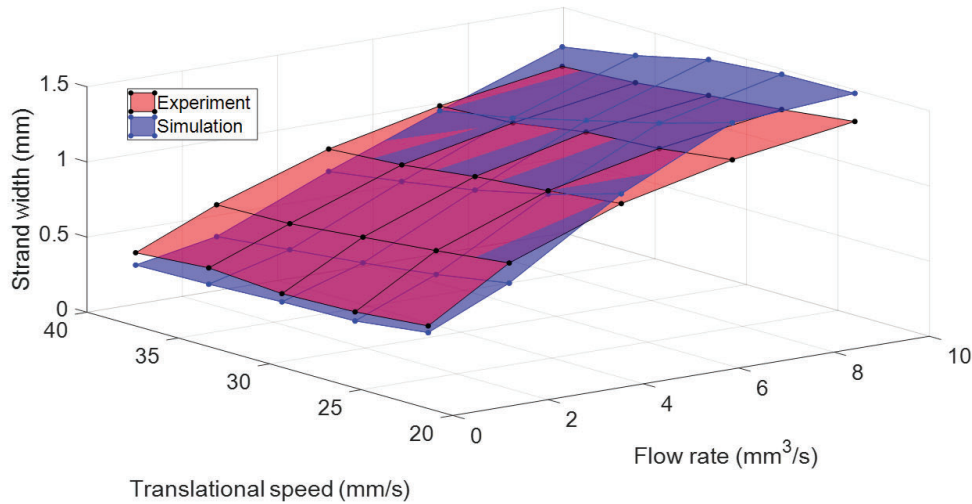

Fig. 13 Experimental validation

6. Conclusion

In this study, a CFD model for simulating the single track deposition of liquid strands in a polymer dispensing system has been developed. A model mesh sensitivity study has been performed to identify the appropriate mesh size. Single track deposition experiments have been carried out for model validation. The model is found to be effective in predicting the strand width, e.g., the maximum error is ~37% and the minimum error is ~2.4%. The findings are summarized below:

(1) The influence of material properties, such as contact angle, surface tension and viscosity on the strand width were studied and linear relationships were established for strand widths and material properties.

(2) Both translational speed and flow rate were found to be important in determining the strand width. Specifically, the increase of translational speed will decrease the strand width while the increase of flow rate will increase the strand width.

(3) A process-quality map was established. According to the map, a constant strand width can be obtained by combining different translational speeds and flow rates. In addition, the process parameters should be selected carefully to avoid defect zones.

7. References

[1] H. Bikas, Panagiotis Stavropoulos, and George Chryssolouris. "Additive manufacturing methods and modelling approaches: a critical review." *The International Journal of Advanced Manufacturing Technology* 83, no. 1-4 (2016): 389-405.

[2] Haiyang He, Jie Xu, Xiaoming Yu, and Yayue Pan. "Effect of Constrained Surface Texturing on Separation Force in Projection Stereolithography." *Journal of Manufacturing Science and Engineering* 140, no. 9 (2018): 091007.

[3] Haiyang He, Yayue Pan, Alan Feinerman, and Jie Xu. "Air-Diffusion-Channel Constrained Surface Based Stereolithography for Three-Dimensional Printing of Objects With Wide Solid Cross Sections." *Journal of Manufacturing Science and Engineering* 140, no. 6 (2018): 061011.

[4] Ian Gibson, David W. Rosen, and Brent Stucker. "Additive manufacturing technologies." Vol. 17. New York: Springer, 2014.

[5] Jacob P. Moore, and Christopher B. Williams. "Fatigue properties of parts printed by PolyJet material jetting." *Rapid Prototyping Journal* 21, no. 6 (2015): 675-685.

[6] Yee Ling Yap, Chengcheng Wang, Swee Leong Sing, Vishwesh Dikshit, Wai Yee Yeong, and Jun Wei. "Material jetting additive manufacturing: An experimental study using designed metrological benchmarks." *Precision engineering* 50 (2017): 275-285.

[7] Farzad Liravi, Robin Darleux, and Ehsan Toyserkani. "Additive manufacturing of 3D structures with non-Newtonian highly viscous fluids: Finite element modeling and experimental validation." *Additive Manufacturing* 13 (2017): 113-123.

[8] X. B. Chen, W. J. Zhang, G. Schoenau, and B. Surgenor. "Off-line control of time-pressure dispensing processes for electronics packaging." *IEEE Transactions on Electronics Packaging Manufacturing* 26, no. 4 (2003): 286-293.

[9] Li Jianping, and Deng Guiling. "Technology development and basic theory study of fluid dispensing-a review." In *Proceedings of the Sixth IEEE CPMT Conference on High Density Microsystem Design and Packaging and Component Failure Analysis (HDP'04)*, pp. 198-205. IEEE, 2004.

[10] X. B. Chen, G. Shoenau, and W. J. Zhang. "Modeling of time-pressure fluid dispensing processes." *IEEE Transactions on Electronics Packaging Manufacturing* 23, no. 4 (2000): 300-305.

[11] Bo Cheng, Xiaobai Li, Charles Tuffile, Alexander Ilin, Hannes Willeck, and Udo Hartel. "Multi-physics modeling of single track scanning in selective laser melting: powder compaction effect." *In 29th Annual International Solid Freeform Fabrication Symposium – An Additive Manufacturing Conference*, Austin, TX, USA, August 13-15, 2018, pp. 1887-1902.

[12] Haiyang He, Yang Yang, and Yayue Pan. "Machine learning for continuous liquid interface production: Printing speed modelling." *Journal of Manufacturing Systems* 50 (2019): 236-246.

[13] Raphaël Comminal, Marcin P. Serdeczny, David B. Pedersen, and Jon Spangenberg. "Numerical modeling of the strand deposition flow in extrusion-based additive manufacturing." *Additive Manufacturing* 20 (2018): 68-76.

[14] Marcin P. Serdeczny, Raphaël Comminal, David B. Pedersen, and Jon Spangenberg. "Numerical prediction of the porosity of parts fabricated with fused deposition modeling." *In 29th Annual International Solid Freeform Fabrication Symposium – An Additive Manufacturing Conference*, Austin, TX, USA, August 13-15, 2018.

[15] Marcin P. Serdeczny, Raphael Comminal, David B. Pedersen, and Jon Spangenberg. "Experimental validation of a numerical model for the strand shape in material extrusion additive manufacturing." *Additive Manufacturing* 24 (2018): 145-153.

[16] Mihaela Vlasea, and Ehsan Toyserkani. "Experimental characterization and numerical modeling of a micro-syringe deposition system for dispensing sacrificial photopolymers on particulate ceramic substrates." *Journal of Materials Processing Technology* 213, no. 11 (2013): 1970-1977.

[17] S. Boonsang, and W. Lertkittiwattanakul. "A flash photography method for the measurements of the fluid flow dynamic of a fluid dispensing system." *Measurement* 102 (2017): 57-63.

[18] Blake P. Heller, Douglas E. Smith, and David A. Jack. "Planar deposition flow modeling of fiber filled composites in large area additive manufacturing." *Additive Manufacturing* 25 (2019): 227-238.

[19] ANSYS Fluent documentation